

# Casimir-Polder energy level shifts of an out-of-equilibrium particle near a microsphere

Simen Å. Ellingsen

*Department of Energy and Process Engineering, Norwegian University of Science and Technology, N-7491 Trondheim, Norway*

Stefan Yoshi Buhmann and Stefan Scheel

*Quantum Optics and Laser Science, Blackett Laboratory, Imperial College London,  
Prince Consort Road, London SW7 2BW, United Kingdom*

(Dated: November 21, 2018)

Rydberg atoms and beams of ultracold polar molecules have become highly useful experimental tools in recent years. There is therefore a need for accessible calculations of interaction potentials between such particles and nearby surfaces and structures, bearing in mind that the particles are far out of thermal equilibrium with their environment and that their interaction is predominantly non-retarded. Based on a new perturbative expansion with respect to the inverse speed of light and the inverse conductivity, we derive a simple, closed-form expression for the interaction potential (i.e., the particle energy level shifts) of a particle and a metallic sphere that is accurate at better than 1% level for typical experimental set-ups at room temperature and above, and off by no more than a few percent at any temperature including zero. Our result illuminates the influence of retardation and imperfect conductivity and the interplay of these effects with geometry. The method developed for the present study may be applied to other, more complex geometries.

PACS numbers: 31.30.jh, 12.20.-m, 34.35.+a, 42.50.Nn

## I. INTRODUCTION

Recent times have witnessed a blossoming of experimental set-ups in which the detailed interaction of particles with nearby surfaces, in particular the Casimir-Polder (retarded van der Waals) [1] interaction, is important. Some such systems are typically far out of thermal equilibrium, such as Bose-Einstein condensates in magnetic traps close to surfaces, beams of cold polar molecules and Rydberg atoms. We shall focus on the two latter categories herein. For example, the interaction between Rydberg atoms [2] and surfaces are essential to the understanding of the behavior of Rydberg atoms in vapour cells [3] and near atom chips [4], systems which have already been investigated in several experiments. Various suggested mechanisms for quantum information processing also involve Rydberg atoms close to metallic surfaces [5–7]. Moreover, beams of cold polar molecules have already been put to use in a range of experimental applications as reviewed in Refs [8–10]. For instance, trapping of cold CO molecules near atom chips using electric traps has recently been realized [11].

We derive herein a simple closed form expression for the CP interaction between a particle and a sphere valid both for Rydberg atoms and cold molecules. Second only to the plane surface, the spherical geometry is arguably the most generically useful to consider in all microscopic applications. The microsphere is the standard vehicle in the rapidly progressing field of micromanipulation and photonics, a field closely bordering on atomic physics where CP forces are of importance. Using laser beams, microspheres can be trapped and pushed [12] and perhaps even pulled [13] for detailed manipulation, and are readily transported along optical fibres via the evanescent field [14]. Microsphere optical resonators with extremely

high Q-factors have been built, and are useful e.g. for low threshold lasing [15]. Our closed form expression, not involving the typical lengthy sums of Mie scattering coefficients, is immediately useful for direct insertion into numerical simulations of microsystems, as well as analysis of experimental data.

Rydberg atoms and cold (ground state) polar molecules share two traits that set them sharply apart from the ground state or thermalized atoms which have typically been considered in the van der Waals and Casimir-Polder (CP) literature. Firstly, they are both far out of thermal equilibrium with their thermal environment. Rydberg atoms have been excited to a high principal quantum number, far from an atom's thermalized state, which is almost identical to its ground state since excitation energies are large compared to  $k_B T$  (room temperature assumed). The excitation energies of rovibrational states of molecules, in contrast, are small compared to  $k_B T$ , so a thermalized molecule significantly occupies a number of its energy eigenstates. Thus also ground state molecules at room temperature are far from thermal equilibrium. Systems with magnetic transitions exhibit similar properties [16].

Secondly, and for the same reason, the Casimir-Polder interaction between these particles and nearby surfaces is predominantly non-retarded, and retardation corrections due to the finite speed of light enter only as a correction. Typically, the retarded interaction regime stretches for tens and hundreds of micrometers for polar molecules and Rydberg atoms, respectively [17, 18], thus including the separations normally encountered in experiments and applications.

Whereas thermal non-equilibrium initially complicates theoretical treatment, the non-retardedness of the interaction introduces a significant simplification, allowing al-

most surprisingly simple results to be achieved. The general theory for Casimir-Polder interactions of a particle in an arbitrary superposition of eigenstates was recently derived by some of us [19], and has since been applied to planar geometries for Rydberg atoms and molecules [18, 20]. Strikingly, it was found that for non-retarded interaction with a flat metallic surface the interaction potential is virtually independent of temperature [21], a result that can be extended to arbitrary geometries [22]. For a full theoretical background of different non-equilibrium CP scenarios the reader may additionally refer to Refs. [23–29]. The theories for different non-equilibrium situations, albeit apparently disparate, may be shown to concord as they should [30].

We consider the general situation of a particle whose eigenstates are  $|n\rangle$ . It was shown in Ref. [19] that for a particle prepared in an arbitrary superposition of eigenstates  $|\phi\rangle = \sum_n p_n |n\rangle$  with occupation probabilities  $p_n$ , the Casimir-Polder potential may be written as a sum over transitions between pairs of eigenstates according to

$$U_\phi = \sum_n p_n U_n \quad (1.1)$$

with

$$U_n = \sum_k U_{nk} \quad (1.2)$$

where the sum runs over all other eigenstates  $|k\rangle$  to which there is an allowed dipole transition.

Crucial to the understanding of the CP interactions of both cold molecules [20] and Rydberg atoms [18] is the realization that only a few transitions turn out to give significant contributions. To wit, the important transitions were found to be those corresponding to the smallest difference in eigenenergy  $\Delta E_{kn} = E_k - E_n$ , i.e. the smallest transition frequency  $\omega_{kn} = \Delta E_{kn}/\hbar$  or correspondingly the longest transition wavelength  $\lambda_{kn} = 2\pi c/\omega_{kn}$ . For example, a Rydberg atom near a half-space prepared in an  $s$ -state of principal quantum number  $n$ , obtains significant contributions from transitions to the few different  $p$ -states of principal quantum numbers  $n$  and  $n-1$  [18]; for ground state LiH molecules the only significant transition was to the lowest rotational state, whereas for YbF also the first vibrational state was required [20]. Transitions with larger  $\Delta E_{kn}$  could be ignored to a good approximation.

Because of this fact the typical values of  $\lambda_{kn}$  for cold polar molecules and Rydberg atoms alike are usually much larger than the typical distance  $z$  from the particle to a nearby body in experiments involving surfaces. In other words, for the dominating transitions  $|n\rangle \rightarrow |k\rangle$ ,

$$\frac{z}{\lambda_{kn}} = \frac{\omega_{kn} z}{2\pi c} \ll 1, \quad (1.3)$$

hence the interaction is essentially *non-retarded*.

Recently we found that in the non-retarded regime the CP interaction near a metallic half-space is virtually temperature independent [21]. The thermal CP potential then agrees with its zero-temperature counterpart for all temperatures. This was later shown to be a reasonable approximation for bodies of arbitrary shape [22]. Temperature-dependent corrections to the zero-temperature potential were identified to stem from retardation and imperfect conductivity. The magnitude of the latter corrections were found to strongly depend on the body shape and curvature, demonstrating that geometry and temperature are closely intertwined [31]. It is therefore necessary in practice to study different geometries individually.

The case of an atom interacting with a metal sphere to be studied is a prototype of a body with a curved surface. Various embodiments of the particle-sphere interactions at zero temperature have been treated by a number of authors [32–39]. In most of these works, the CP potential is obtained from a numerical computation which suffers from poor convergence at small curvatures. In contrast, we will derive an approximate analytical result based on a perturbative expansion that is readily accessible while illuminating the impact of retardation and imperfect reflection as well as the interplay of these factors with geometry: We calculate the CP potential contribution from transition  $|n\rangle \rightarrow |k\rangle$  under the relevant assumption of non-retarded interaction, Eq. (1.3), which we quantify by a retardation parameter

$$x = \frac{r\omega_{kn}}{c} \ll 1 \quad (1.4)$$

where  $r$  is distance from the particle to the sphere's center. We quote here the final result, to be derived below, for the thermal Casimir-Polder potential of an atom at distance  $r$  from the center of a metal sphere of radius  $R$ :

---


$$U_{nk}(r) = -\frac{|\mathbf{d}_{kn}|^2}{24\pi\epsilon_0 r^3} \frac{\phi^3(6-3\phi^2+\phi^4)}{(1-\phi^2)^3} + \frac{|\mathbf{d}_{kn}|^2}{24\pi\epsilon_0 r^3} \left( \frac{k_B T}{\hbar\omega_{kn}} - \frac{1}{2} \right) \left\{ x^2 [3(1+3\phi^4)\text{artanh}\phi - \phi(3-\phi^2)] \right. \\ \left. + 2\phi^3 \log(1-\phi^2) \right\} + 2x\phi^2 \text{Re} \left\{ \frac{i}{\sqrt{\epsilon(\omega)}} \right\} \left[ \frac{3+7\phi^2-4\phi^4}{(1-\phi^2)^2} - \log(1-\phi^2) \right] + \dots + \mathcal{O}(T^{-1}) \quad (1.5)$$

where we have introduced the dimensionless geometry parameter

$$\phi = R/r. \quad (1.6)$$

The expression (1.5) is remarkably simple compared to a numerical evaluation of the starting equations, involving infinite sums over Mie scattering coefficients. It holds when  $x \ll 1$ , but  $\text{Im}\{\sqrt{\varepsilon}\}x\phi = \text{Im}\{\sqrt{\varepsilon}\}\omega_{kn}R/c$  still significantly exceeds unity, which is the case for good conductors in combination with typical values of  $x$  for the systems under consideration. The dots indicate higher-order contributions in the small parameters  $x$  and  $1/(x\sqrt{\varepsilon})$ . For definitions of the various quantities in Eq. (1.5), see Sec. II below.

In the following we derive the CP potential for a particle near a metallic sphere including the leading correction for small  $x$  (retardation correction) and  $1/(x\sqrt{\varepsilon})$  (imperfect reflectivity correction), starting from the general CP theory for particles out of thermal equilibrium, which is outlined in Section II. Our method may in principle be employed for any geometry to derive perturbative temperature corrections such as that presented herein. Explicit corrections for the particle–sphere configuration are derived in Section III and analysed in Section III C.

## II. GENERAL FORMALISM

The general formalism for the temperature-dependent CP force on a particle in an energy eigenstate is found in Ref. [19]. Here we shall restrict our attention to the special case of an isotropic particle. As explained above, the potential on a Rydberg atom or cold molecule alike takes form of a sum over just a few contributions from pairs of eigenstates which all have transition wavelengths in the same order of magnitude. It is sufficient therefore to consider a single transition  $|n\rangle \rightarrow |k\rangle$ . Our considerations for one such transition will therefore hold for all relevant transitions, and all that is required in order to return to the full description of these particles is to sum the final result over the relevant transitions according to Eq. (1.2). The generalisation to anisotropic particles is straightforward (cf. Refs [19, 22]).

This section reviews the general framework for treating the small temperature correction in the non-resonant regime for arbitrary geometries, which we apply below to a metal sphere. In the notation of Ref. [22], the CP potential of an isotropic non-magnetic particle in state  $|n\rangle$  due to a possible transition to state  $|k\rangle$  splits naturally into a non-resonant (nr) and a resonant (r) part [19]

$$U_{nk}(\mathbf{r}) = U_{nk}^{\text{nr}}(\mathbf{r}) + U_{nk}^{\text{r}}(\mathbf{r}), \quad (2.1)$$

where the two parts are given by

$$U_{nk}^{\text{nr}}(\mathbf{r}) = -\frac{2k_{\text{B}}T|\mathbf{d}_{nk}|^2\omega_{kn}}{3\hbar\varepsilon_0} \sum_{j=0}^{\infty} \frac{\Gamma_{i\xi_j}(\mathbf{r})}{\omega_{kn}^2 + \xi_j^2}; \quad (2.2a)$$

$$U_{nk}^{\text{r}}(\mathbf{r}) = \frac{|\mathbf{d}_{kn}|^2}{3\varepsilon_0} n(\omega_{kn}) \text{Re} \Gamma_{\omega_{kn}}(\mathbf{r}). \quad (2.2b)$$

Here,  $\mathbf{d}_{kn} = \langle k|\mathbf{d}|n\rangle$  is the transition dipole matrix element and

$$\xi_j = 2\pi j k_{\text{B}}T/\hbar \quad (2.3)$$

are the Matsubara frequencies. The photon number at frequency  $\omega$  and temperature  $T$  is given by the Bose-Einstein distribution,

$$n(\omega) = \frac{1}{\exp(\hbar\omega/k_{\text{B}}T) - 1} = -[n(-\omega) + 1]. \quad (2.4)$$

The function

$$\Gamma_{\omega}(\mathbf{r}) \equiv \frac{\omega^2}{c^2} \lim_{\mathbf{r}' \rightarrow \mathbf{r}} \text{tr} \mathbf{G}^{(1)}(\mathbf{r}, \mathbf{r}', \omega) \quad (2.5)$$

is given in terms of the scattering part  $\mathbf{G}^{(1)}$  of the total dyadic Green's function satisfying

$$\left[ \nabla \times \nabla \times - \frac{\omega^2}{c^2} \varepsilon(\mathbf{r}, \omega) \right] \mathbf{G}(\mathbf{r}, \mathbf{r}', \omega) = \delta(\mathbf{r} - \mathbf{r}') \mathbf{1}. \quad (2.6)$$

( $\mathbf{1}$ : unit tensor). The relative permittivity  $\varepsilon(\mathbf{r}, \omega)$  of the present bodies is isotropic and we have assumed the bodies to be non-magnetic. Due to causality,  $\Gamma_{i\xi_j}$  is real, being a generalized susceptibility evaluated at imaginary frequency, so in particular  $\Gamma_{i0} = \Gamma_0$  is real.

In the following, we consider a single transition  $|n\rangle \rightarrow |k\rangle$  and simplify our notation according to

$$|\mathbf{d}_{kn}|^2 \rightarrow |\mathbf{d}|^2; \quad \omega_{kn} \rightarrow \omega; \quad U_{nk}(\mathbf{r}) \rightarrow U(\mathbf{r}).$$

Note that  $\omega$  can be either positive or negative depending on whether the transition is upwards or downwards.

Knowing that the potential is largely temperature independent through the non-retarded region, consider for now the regime in which the linear  $T$ -corrections becomes important, i.e., the spectroscopic high-temperature regime,

$$k_{\text{B}}T \gg \hbar\omega.$$

Here, the contribution of the lowest Matsubara frequency ( $j = 0$ ) dominates in Eq. (2.2a), so

$$U^{\text{nr}}(\mathbf{r}) = -\frac{|\mathbf{d}|^2 k_{\text{B}}T}{3\varepsilon_0 \hbar\omega} \Gamma_0(\mathbf{r}) + \mathcal{O}(T^{-1}). \quad (2.7)$$

The photon number in this regime is

$$n(\omega) = \frac{k_{\text{B}}T}{\hbar\omega} - \frac{1}{2} + \mathcal{O}(T^{-1}), \quad (2.8)$$

so the resonant potential (2.2b) reads

$$U^{\text{r}}(\mathbf{r}) = \frac{|\mathbf{d}|^2}{3\varepsilon_0} \left( \frac{k_{\text{B}}T}{\hbar\omega} - \frac{1}{2} \right) \text{Re} \Gamma_{\omega}(\mathbf{r}). \quad (2.9)$$

Combining these results, we find for the full potential in the spectroscopic high-temperature regime that

$$U(\mathbf{r}) = -\frac{|\mathbf{d}|^2}{6\varepsilon_0} \Gamma_0(\mathbf{r}) + \frac{|\mathbf{d}|^2}{3\varepsilon_0} \left( \frac{k_{\text{B}}T}{\hbar\omega} - \frac{1}{2} \right) \text{Re} \Delta \Gamma_{\omega}(\mathbf{r}) + \mathcal{O}(T^{-1}) \quad (2.10)$$

where  $\Delta\Gamma_\omega = \Gamma_\omega - \Gamma_0$ .

For comparison, in the zero-temperature limit, in which the Matsubara sum becomes an integral according to standard procedures (e.g. the Euler-Maclaurin formula), one obtains

$$U(\mathbf{r})|_{T=0} = -\frac{|\mathbf{d}|^2\omega}{3\pi\varepsilon_0} \int_0^\infty d\xi \frac{\text{tr}\Gamma_{i\xi}^{(1)}(\mathbf{r})}{\omega^2 + \xi^2} - \frac{|\mathbf{d}|^2}{3\varepsilon_0} \Theta(-\omega)\text{Re}\Gamma_\omega(\mathbf{r}) \quad (2.11)$$

with  $\Theta(x)$  denoting the unit step function.

In the nonretarded and perfect-conductor limits, we have  $\Gamma_{i\xi}(\mathbf{r}) \simeq \text{Re}\Gamma_\omega(\mathbf{r}) \simeq \Gamma_0(\mathbf{r})$  [21] which implies  $\text{Re}\Delta\Gamma_\omega(\mathbf{r}) \simeq 0$ . In this case, both Eqs. (2.10) and (2.11) reduce to

$$U_0(\mathbf{r}) = -\frac{|\mathbf{d}|^2}{6\varepsilon_0}\Gamma_0(\mathbf{r}) \quad (2.12)$$

and the CP potential is independent of temperature throughout.

In this article, we are interested in the corrections to the temperature-independent result (2.12) that arise due to small violations of the non-retarded limit and perfect reflectivity. As seen from Eq. (2.10), they are governed by  $\text{Re}\Delta\Gamma_\omega(\mathbf{r})$ . When all present macroscopic bodies are perfectly conducting (PC), then  $\Gamma_\omega$  satisfies [22]

$$\Gamma_\omega^{\text{PC}} = \Gamma_0^{\text{PC}} + \frac{\omega^2}{2c^2} \frac{d^2\Gamma_\omega^{\text{PC}}}{d\omega^2} \Big|_{\omega=0} + \dots; \quad \omega \rightarrow 0, \quad (2.13)$$

so that

$$\Delta\Gamma_\omega^{\text{PC}} \approx \frac{\omega^2}{2c^2} \frac{d^2\Gamma_\omega^{\text{PC}}}{d\omega^2} \Big|_{\omega=0}; \quad \omega \rightarrow 0, \quad (2.14)$$

is quadratic in  $\omega$ . This correction accounts for the fact that electromagnetic interactions are transmitted at the finite speed of light; we will refer to it as the retardation correction in the following.

For an imperfect conductor, the corrections to the Green's function for small frequencies includes a second correction due to the frequency-dependence of the reflectivity of the bodies. We write

$$\Delta\Gamma_\omega = \Delta\Gamma_\omega^{\text{ret.}} + \Delta\Gamma_\omega^{\text{refl.}} \quad (2.15)$$

due to retardation and reflectivity, respectively. When treating  $\omega$  and  $\varepsilon(\omega)$  as independent variables, the retardation correction  $\Delta\Gamma_\omega^{\text{ret.}}$  is the leading-order term in  $1/\sqrt{\varepsilon(\omega)}$  and next-to-leading in  $\omega$ ; whereas the reflectivity correction  $\Delta\Gamma_\omega^{\text{refl.}}$  is the contribution sub-leading in  $1/\sqrt{\varepsilon(\omega)}$  and leading in  $\omega$ . Note that the perfect-conductor limit  $|\varepsilon(\omega)| \rightarrow \infty$  does not commute with the nonretarded limit  $\omega \rightarrow 0$  in this case. The incompatibility of the two limits was first pointed out in Ref. [40] and is at the heart of the debate over the temperature correction to the Casimir effect [41]. For a metal body at typical frequencies and distances, the perfect-conductor

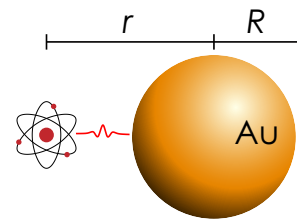


FIG. 1: The geometry considered: a quantum particle prepared in eigenstate  $|n\rangle$  outside a gold sphere.

limit has to be performed before the nonretarded limit, see Sect. III below.

With the leading corrections to the Green's function being given by Eq. (2.15), the thermal CP potential (2.12) can be given as

$$U(\mathbf{r}) = U_0(\mathbf{r}) + \Delta U_{\text{ret.}}(\mathbf{r}) + \Delta U_{\text{refl.}}(\mathbf{r}) + \mathcal{O}(T^{-1}) \quad (2.16)$$

with

$$\Delta U_i(\mathbf{r}) = \frac{|\mathbf{d}|^2}{3\varepsilon_0} \left( \frac{k_B T}{\hbar\omega} - \frac{1}{2} \right) \text{Re}\Delta\Gamma_\omega^i(\mathbf{r}), \quad (2.17)$$

$i = \text{ret.}, \text{refl.}$  The relative corrections due to retardation and reflection read

$$\frac{\Delta U_i(\mathbf{r})}{U_0(\mathbf{r})} = -2 \left( \frac{k_B T}{\hbar\omega} - \frac{1}{2} \right) \frac{\text{Re}\Delta\Gamma_\omega^i(\mathbf{r})}{\Gamma_0(\mathbf{r})}. \quad (2.18)$$

Note that  $\text{Re}\Delta\Gamma_\omega(\mathbf{r})$  is an even function of  $\omega$ , as follows directly from definition (2.5) together with the Schwarz reflection principle  $\mathbf{G}(\mathbf{r}, \mathbf{r}'; -\omega) = \mathbf{G}^*(\mathbf{r}, \mathbf{r}'; \omega)$ . As a consequence, the leading temperature corrections in the high-temperature limit, being proportional to  $\text{Re}\Delta\Gamma_\omega(\mathbf{r})/\omega$ , change sign when comparing downward and upward transitions.

### III. CASIMIR-POLDER POTENTIAL NEAR A SPHERE

As depicted in Fig. 1, we consider a particle at distance  $r$  from the center of a sphere of radius  $R$  and permittivity  $\varepsilon = \varepsilon(\omega)$ . The dyadic Green's function leads to [37]

$$\Gamma_\omega(\mathbf{r}) = \frac{i\mathbf{x}}{4\pi r^3} \sum_{l=1}^{\infty} (2l+1) \left\{ x^2 r_l^{\text{TE}}(\phi x) h_l^{(1)}(x)^2 + r_l^{\text{TM}}(\phi x) \left[ l(l+1) h_l^{(1)}(x)^2 + \tilde{h}_l^{(1)\prime}(x)^2 \right] \right\} \quad (3.1)$$

where  $h_l^{(1)}(x)$  is the spherical Hankel function of the first kind,  $\tilde{h}_l^{(1)\prime}(x)$  [and for future reference,  $\tilde{j}_l'(x)$ ] is shorthand for

$$\tilde{h}_l^{(1)\prime}(x) = [x h_l^{(1)}(x)]'; \quad \tilde{j}_l'(x) = [x j_l(x)]' \quad (3.2)$$

[ $j_l(x)$ : spherical Bessel function of the first kind]. For convenience we are using the dimensionless distance and

size parameters  $x = r\omega/c$  and  $0 < \phi = R/r < 1$ , recall Eqs. (1.4) and (1.6). The reflection coefficients for TE and TM-polarized waves read

$$r_l^{\text{TE}}(z) = -\frac{\tilde{J}_l'(z)j_l(\sqrt{\varepsilon}z) - \tilde{J}_l(\sqrt{\varepsilon}z)j_l'(z)}{\tilde{h}_l^{(1)'}(z)j_l(\sqrt{\varepsilon}z) - \tilde{J}_l(\sqrt{\varepsilon}z)h_l^{(1)'}(z)}; \quad (3.3a)$$

$$r_l^{\text{TM}}(z) = -\frac{\varepsilon\tilde{J}_l'(z)j_l(\sqrt{\varepsilon}z) - \tilde{J}_l(\sqrt{\varepsilon}z)j_l'(z)}{\varepsilon\tilde{h}_l^{(1)'}(z)j_l(\sqrt{\varepsilon}z) - \tilde{J}_l(\sqrt{\varepsilon}z)h_l^{(1)'}(z)}. \quad (3.3b)$$

In the following we assume both the particle-center separation and the sphere size to be non-retarded,  $\phi x \leq x \ll 1$ . In addition, we perform the perfect-conductor limit  $|\varepsilon| \gg 1$ . To leading order, the two limits commute: Taking the perfect-conductor limit first, the reflection coefficients reduce to

$$r_l^{\text{TE}}(\phi x) \xrightarrow{\varepsilon \rightarrow \infty} r_l^{\text{TE,PC}}(\phi x) = -\frac{j_l(\phi x)}{h_l^{(1)}(\phi x)}; \quad (3.4)$$

$$r_l^{\text{TM}}(\phi x) \xrightarrow{\varepsilon \rightarrow \infty} r_l^{\text{TM,PC}}(\phi x) = -\frac{\tilde{J}_l'(\phi x)}{\tilde{h}_l^{(1)'}(\phi x)}, \quad (3.5)$$

see the asymptotes (A1) and (A2) in App. A. Using the expansions (A3) and (A4), they further simplify to

$$r_l^{\text{TE,PC}}(\phi x) \xrightarrow{\phi x \rightarrow 0} r_{l,0}^{\text{TE,PC}}(\phi x) = -\frac{i(\phi x)^{2l+1}}{(2l+1)!!(2l-1)!!}; \quad (3.6)$$

$$r_l^{\text{TM,PC}}(\phi x) \xrightarrow{\phi x \rightarrow 0} r_{l,0}^{\text{TM,PC}}(\phi x) = \frac{l+1}{l} \frac{i(\phi x)^{2l+1}}{(2l+1)!!(2l-1)!!} \quad (3.7)$$

in the non-retarded limit. Here,  $(2l+1)!! = 1 \cdot 3 \cdots (2l+1)$ .

In contrast, when taking the non-retarded limit first, one finds

$$r_l^{\text{TE}}(\phi x) \xrightarrow{\phi x \rightarrow 0} r_{l,0}^{\text{TE}}(\phi x) = (\varepsilon - 1) \frac{i(\phi x)^{2l+3}}{(2l+3)!!(2l+1)!!}; \quad (3.8)$$

$$r_l^{\text{TM}}(\phi x) \xrightarrow{\phi x \rightarrow 0} r_{l,0}^{\text{TM}}(\phi x) = \frac{(l+1)(\varepsilon - 1)i(\phi x)^{2l+1}}{(l\varepsilon + l + 1)(2l+1)!!(2l-1)!!}, \quad (3.9)$$

and subsequently

$$r_{l,0}^{\text{TE}}(\phi x) \xrightarrow{\varepsilon \rightarrow \infty} \varepsilon \frac{i(\phi x)^{2l+3}}{(2l+3)!!(2l+1)!!}; \quad (3.10)$$

$$r_{l,0}^{\text{TM}}(\phi x) \xrightarrow{\varepsilon \rightarrow \infty} \frac{l+1}{l} \frac{i(\phi x)^{2l+1}}{(2l+1)!!(2l-1)!!}. \quad (3.11)$$

While the TM-coefficient takes the same form regardless of the order of the limits, the TE-coefficient yields different results, depending on which of the two limits is performed first.

However, the Green tensor in the non-retarded limit is dominated by  $r_l^{\text{TM}}$ . Substituting the results for the reflection coefficients into (3.1), using the approximation (A4)

from App. A and retaining only the leading order in  $x$ , one finds

$$\Gamma_0^{\text{PC}}(\mathbf{r}) = \frac{1}{4\pi r^3} \sum_{l=1}^{\infty} (2l+1)(l+1)\phi^{2l+1} \\ = \frac{1}{4\pi r^3} \frac{\phi^3(6 - 3\phi^2 + \phi^4)}{(1 - \phi^2)^3}. \quad (3.12)$$

With this result, the temperature-invariant CP potential (2.12) reads

$$U_0(\mathbf{r}) = -\frac{|\mathbf{d}|^2}{24\pi\varepsilon_0 r^3} f(\phi) \quad (3.13)$$

with

$$f(\phi) = \frac{\phi^3(6 - 3\phi^2 + \phi^4)}{(1 - \phi^2)^3} \rightarrow \begin{cases} 6\phi^3 & \text{for } \phi \rightarrow 0, \\ \frac{1}{2(1 - \phi)^3} & \text{for } \phi \rightarrow 1. \end{cases} \quad (3.14)$$

This is in agreement with the zero-temperature potential as found in Ref. [38] for a perfectly conducting sphere in the non-retarded limit on the basis of image-charge techniques. As discussed in Ref. [42], the atom-sphere geometry is a particular example of a two-parameter geometry, conveniently described by a scaling function  $f(\phi)$ .

The accuracy of the simplest, temperature-independent approximation, Eq. (3.13), is demonstrated numerically in Fig. 2 (dashed lines) for a ground-state two-level particle outside a gold sphere. The permittivity of the sphere has been described by a Drude model  $\varepsilon(\omega) = 1 - \omega_P^2/[\omega(\omega + i\gamma)]$  with parameters  $\omega_P = 9\text{eV}$  and  $\gamma = 35\text{meV}$ . For comparison, the same situation but with a smaller sphere is shown in Fig. 3. We see that Eq. (3.13) yields a very good approximation. The exact potential is slightly smaller by at most 5% for  $r\omega/c = 0.1$ . Recall that the leading correction in the high-temperature limit has opposite signs for ground-state and excited atoms. For an excited two-level atom, we would hence find that the exact potential is slightly larger than its approximation (3.13). In the following, we derive analytical expressions for the leading temperature-dependent corrections to Eq. (3.13) providing an even much improved approximation at higher temperatures.

## A. Correction from retardation

When considering the full thermal CP potential (2.2a) and (2.2b) using the Green's function of Eq. (3.1), the non-retarded and perfect-conductor limits do not commute. We have  $\phi x \leq x \ll 1$  and  $|\varepsilon| \gg 1$ , which is compatible with both large and small values of  $|\sqrt{\varepsilon}|\phi x$ . For a metal sphere at typical experimental distances of order micrometers and  $x \sim 0.01 - 0.001$ , we have  $\text{Im}\sqrt{\varepsilon}\phi x \gg 1$ , meaning that the perfect-conductor limit has to be applied first. The opposite limit  $|\sqrt{\varepsilon}|\phi x \ll 1$  may be realised for dielectrics whose permittivity tends to some

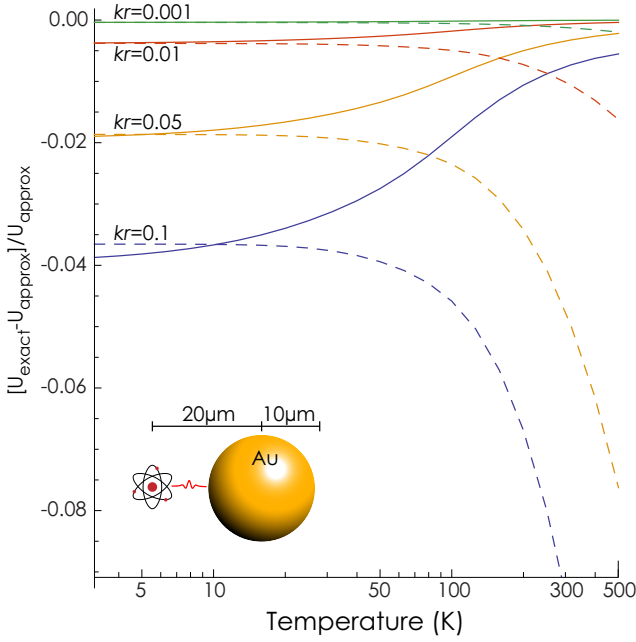


FIG. 2: Numerical comparison of the exact CP potential  $U(T)$  of the contribution from a transition of energy  $\hbar ck$  for a particle outside a gold sphere with  $U_{\text{approx}}$  being respectively the  $T$ -independent result  $U_0$  for a perfect conductor in the non-retarded limit (dashed line) and the approximate expression Eq. (1.5) including the linear temperature correction (solid line). Parameter values:  $R = \frac{1}{2}r = 10\mu\text{m}$ .

moderate electrostatic value, in which case the non-retarded limit would have to be performed first. We briefly consider this case in Appendix B.

The correction from retardation effects is found by using the perfect conductor values (3.4) and (3.5) of the reflection coefficients and expanding  $\Gamma_{\omega}^{\text{PC}}(\mathbf{r})$  as given by Eq. (3.1) in powers of  $x$ , the leading correction term being of order  $x^2$ . We obtain such quadratic corrections from three sources: (A) from the TM-mode reflection coefficient  $r_l^{\text{TM,PC}}$ ; (B) from TM-mode propagators  $h_l^{(1)}(x)^2$  and  $\tilde{h}_l^{(1)'}(x)^2$ ; and (C) from the leading-order TE-mode contribution. The technical details of the small  $x$  expansions of the different cases are found in App.A 1.

As shown therein, correction (A) takes the form

$$r_l^{\text{TM,PC}}(\phi x) = r_{l,0}^{\text{TM,PC}}(\phi x) \left\{ 1 - \frac{(\phi x)^2}{2} \left[ \frac{l+3}{(2l+3)(l+1)} + \frac{l-2}{l(2l-1)} \right] + \dots \right\} \quad (3.15)$$

with  $r_{l,0}^{\text{TM,PC}}$  being given by Eq. (3.7). The correction (B) is found to be

$$r_{l,0}^{\text{TM,PC}}(\phi x) \left[ l(l+1)h_l^{(1)}(x)^2 + \tilde{h}_l^{(1)'}(x)^2 \right] = \frac{(l+1)\phi^{2l+1}}{ix} \left[ 1 + \frac{x^2}{2l+1} + \dots \right]. \quad (3.16)$$

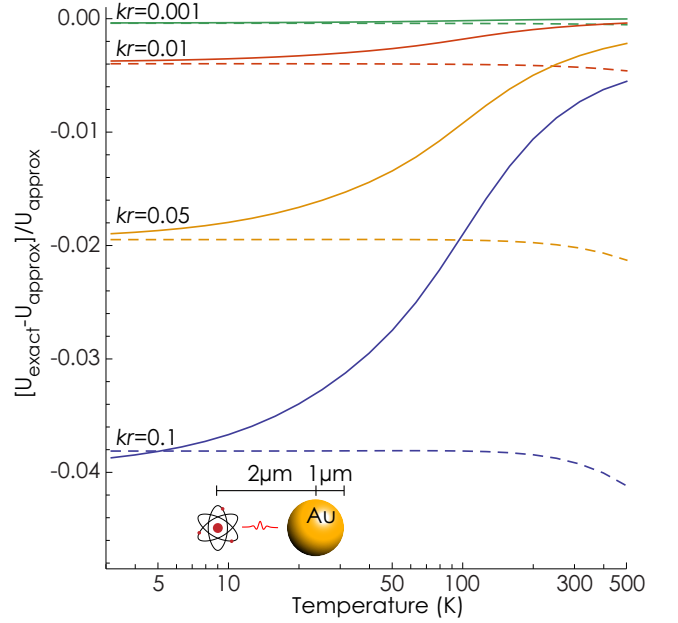


FIG. 3: Same as figure 2, but with a smaller gold sphere:  $R = \frac{1}{2}r = 1\mu\text{m}$ .

Finally, the correction (C) from the TE-mode takes the simple form

$$r_l^{\text{TE,PC}}(\phi x)h_l^{(1)}(x)^2 = -\frac{\phi^{2l+1}}{ix(2l+1)} + \dots \quad (3.17)$$

Substituting these corrections into Eq. (3.1), one finds

$$\Delta\Gamma_{\omega}^{\text{ret.}} = \frac{x^2}{4\pi r^3} \sum_{l=1}^{\infty} \left\{ l\phi^{2l+1} - (2l+1) \left[ \frac{l+3}{2l+3} + \frac{(l+1)(l-2)}{(2l-1)l} \right] \frac{\phi^{2l+3}}{2} \right\} \quad (3.18)$$

The sum may be carried out in closed form by splitting the expressions into partial fractions. One finds

$$\Delta\Gamma_{\omega}^{\text{ret.}} = \frac{x^2}{8\pi r^3} \left[ 3(1+3\phi^4)\text{artanh}\phi - \phi(3-\phi^2) + 2\phi^3 \log(1-\phi^2) \right]. \quad (3.19)$$

Substituting this result into Eq. (2.17), we obtain the retardation correction

$$\Delta U_{\text{ret.}}(\mathbf{r}) = \frac{|\mathbf{d}|^2 x^2}{24\pi\epsilon_0 r^3} \left( \frac{k_{\text{B}}T}{\hbar\omega} - \frac{1}{2} \right) g_{\text{ret.}}(\phi) \quad (3.20)$$

with scaling function

$$g_{\text{ret.}}(\phi) = 3(1+3\phi^4)\text{artanh}\phi - \phi(3-\phi^2) + 2\phi^3 \log(1-\phi^2) \rightarrow \begin{cases} 2\phi^3 & \text{for } \phi \rightarrow 0, \\ -4\log(1-\phi) & \text{for } \phi \rightarrow 1. \end{cases} \quad (3.21)$$

Its relative contribution (2.18) is given by

$$\frac{\Delta U_{\text{ret.}}(\mathbf{r})}{U_0(\mathbf{r})} = - \left( \frac{k_B T}{\hbar \omega} - \frac{1}{2} \right) x^2 \frac{g_{\text{ret.}}(\phi)}{f(\phi)}. \quad (3.22)$$

### B. Correction from imperfect reflection

The leading order corrections to the ideal reflection coefficients are calculated in App. A 2 and have the form

$$r_l^{\text{TE}}(\phi x) = r_{l,0}^{\text{TE,PC}}(\phi x) \left[ 1 - \frac{i(2l+1)}{\sqrt{\varepsilon} \phi x} + \dots \right]; \quad (3.23a)$$

$$r_l^{\text{TM}}(\phi x) = r_{l,0}^{\text{TM,PC}}(\phi x) \left[ 1 + \frac{i \phi x}{\sqrt{\varepsilon}} \frac{2l+1}{l(l+1)} + \dots \right] \quad (3.23b)$$

for  $x \ll 1$ , with  $r_{l,0}^{\text{TE,PC}}$  and  $r_{l,0}^{\text{TM,PC}}$  given by Eqs. (3.6) and (3.7). Substituting these results into Eq. (3.1) and using the leading-order small argument expansions in Eqs. (3.16) and (3.17), we find

$$\begin{aligned} \Delta \Gamma_{\omega}^{\text{refl.}} &= \frac{i x}{4 \pi r^3 \sqrt{\varepsilon}} \sum_{l=1}^{\infty} (2l+1) \left[ 1 + \frac{2l+1}{l} \phi^2 \right] \phi^{2l} \\ &= \frac{i x \phi^2}{4 \pi r^3 \sqrt{\varepsilon}} \left[ \frac{3 + 7\phi^2 - 4\phi^4}{(1 - \phi^2)^2} - \log(1 - \phi^2) \right]. \end{aligned} \quad (3.24)$$

Inserting this into Eq. (2.17), the reflectivity correction is found to be

$$\Delta U_{\text{refl.}}(\mathbf{r}) = \frac{|\mathbf{d}|^2 x}{24 \pi \varepsilon_0 r^3} \text{Re} \left( \frac{i}{\sqrt{\varepsilon}} \right) \left( \frac{k_B T}{\hbar \omega} - \frac{1}{2} \right) g_{\text{refl.}}(\phi) \quad (3.25)$$

with scaling function

$$\begin{aligned} g_{\text{refl.}}(\phi) &= 2\phi^2 \left[ \frac{3 + 7\phi^2 - 4\phi^4}{(1 - \phi^2)^2} - \log(1 - \phi^2) \right] \\ &\rightarrow \begin{cases} 6\phi^2 & \text{for } \phi \rightarrow 0, \\ \frac{3}{(1 - \phi)^2} & \text{for } \phi \rightarrow 1. \end{cases} \end{aligned} \quad (3.26)$$

Its relative contribution (2.18) reads

$$\frac{\Delta U_{\text{refl.}}(\mathbf{r})}{U_0(\mathbf{r})} = - \left( \frac{k_B T}{\hbar \omega} - \frac{1}{2} \right) x \text{Re} \left( \frac{i}{\sqrt{\varepsilon}} \right) \frac{g_{\text{refl.}}(\phi)}{f(\phi)}. \quad (3.27)$$

### C. Discussion and comparison

Combining the  $T$ -invariant result (2.12) with the retardation and reflectivity corrections (3.20) and (3.25), we obtain the weakly temperature-dependent CP potential (1.5), as stated in the introduction. The quality of this analytic high-temperature result is demonstrated in Figs. 2 and 3 (solid lines), where we compare it with the result of an exact numerical calculation for the contribution  $U_{nk}$  [see Eq. (1.2)] from an upward internal energy

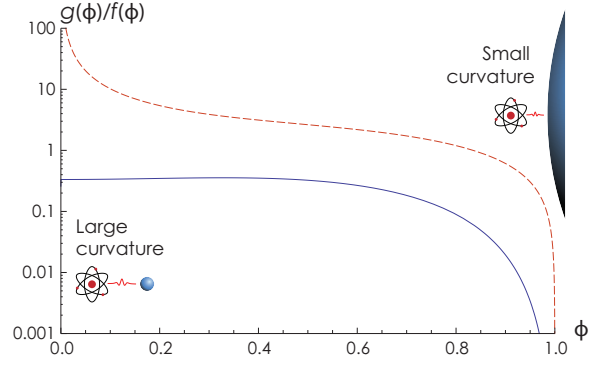


FIG. 4: Ratios of the scaling functions  $g_{\text{ret.}}(\phi)/f(\phi)$  (solid line) and  $g_{\text{refl.}}(\phi)/f(\phi)$  (dashed line) that govern the impact of retardation and finite reflectivity on the thermal CP potential.

transition of a particle outside a gold sphere. One sees that the analytic result is an excellent approximation for temperatures  $T > 200$  K. Notice in particular that for  $x$  of the order 0.1 and lower, Eq. (1.5) is an excellent approximation (better than 1%) at  $T \approx 300$  K, where most experiments are performed.

While the  $T$ -invariant first term in Eq. (1.5) is quite adequate for very small retardation values (such as  $x = 0.001$ , typical of Rydberg atoms), the full expression is much better as  $x$  increases to about 0.1. This could be the case for certain cold polar molecules. For example, with LiH molecules [20],  $x = 0.1$  corresponds to  $r = 15 \mu\text{m}$  for the dominant, rotational transition which is not an atypical situation. In this case the  $T$ -independent term is off by almost 10% at 300 K with the 10 micron sphere, but is still better than 1% when the correction is included. In general, the  $T$ -invariant first term in Eq. (1.5) becomes a worse approximation at higher temperatures, with the error increasing without bounds as the environment temperature rises. In contradistinction, our approximation (1.5) becomes better and better at high temperatures and its error remains bounded throughout.

According to Eqs. (3.22) and (3.27), the relative contributions from retardation and finite reflectivity are governed by the ratios  $g_i(\phi)/f(\phi)$  of the scaling functions as given by Eqs. (3.14), (3.21) and (3.26). These ratios are depicted in Fig. 4. The figure shows that both contributions strongly depend on the curvature of the sphere as parametrised by  $\phi$ . The retardation contribution takes a value  $1/3$  for a strongly curved sphere and stays approximately constant for  $\phi \lesssim 0.5$ . In the limit of a flat surface, it rapidly falls off as  $-4(1 - \phi)^3 \log(1 - \phi)$ . The reflectivity correction grows as  $1/\phi$  in the limit of a strongly curved sphere and falls off gently as  $6(1 - \phi)$  in the limit of a flat surface.

The ratio  $g_{\text{refl.}}(\phi)/f(\phi)$  is greater than  $g_{\text{ret.}}(\phi)/f(\phi)$  by at least an order of magnitude for all curvatures. One has to bear in mind, however, that the reflectivity correction carries an additional factor  $\text{Re}(i/\sqrt{\varepsilon})/x \ll 1$ . For a metal

described by a Drude model with  $\omega, \gamma \ll \omega_P$ , one finds

$$\begin{aligned} \operatorname{Re}[i/\sqrt{\varepsilon(\omega)}] &= \omega_P^{-1} \left[ \frac{1}{2}(\sqrt{\omega^2 + \gamma^2} + |\omega|)|\omega| \right]^{\frac{1}{2}} \\ &\simeq \begin{cases} \sqrt{\omega\gamma/2}/\omega_P & \text{for } \omega \ll \gamma, \\ \omega/\omega_P & \text{for } \omega \gg \gamma. \end{cases} \end{aligned} \quad (3.28)$$

Depending on the actual value of  $\operatorname{Re}(i/\sqrt{\varepsilon})/x \ll 1$  for a given molecule and material, either one of the reflectivity or retardation may dominate for given curvatures. However, the asymptotic behaviour observed in Fig. 4 shows that the reflectivity correction will always dominate in the limits of small or large curvature.

#### IV. SUMMARY

We have studied the temperature-dependent CP potential of a particle strongly out of thermal equilibrium near a metal sphere, and have derived a simple approximate expression in closed form for the interaction potential. The approximation is valid at the 1% or better for Rydberg atoms and cold polar molecules at all temperatures for typical experimental length scales. We have assumed both the particle–sphere distance and the particle’s transition frequency to be small enough so that retardation and imperfect reflectivity present only small perturbations to the temperature-independent result. Such is typically the case in experimental set-ups in which cold polar molecules or Rydberg atoms are used, whose interaction potential is dominated by long wavelength transitions for which the non-retarded regime extends to tens and hundreds of micrometers, respectively.

In recent publications it has been shown that the Casimir–Polder potential acting on a particle prepared in an eigenstate at a non-retarded distance from a macroscopic body can be virtually independent of the surrounding temperature. This is the case for the geometry considered, and the error made in approximating the interaction as independent of temperature from zero to room temperature is only a few percent for sufficiently non-retarded interaction. The small temperature-dependent corrections to the potential of a metal body have been identified to stem from retardation and imperfect reflectivity and we have analysed these separately and discussed the relative importance of each with respect to the other. Our results show that reflectivity is the dominant correction for very large or small curvatures, while intermediate curvatures may be governed by either retardation and reflectivity corrections, depending on particle and material.

The perturbative method employed in this investigation is equally well suited for the study of more complicated geometries. Again, it promises physical insights that are hard or even impossible to gain by numerical means.

We thank Ho Trung Dung for discussions. This work was supported by the UK Engineering and Physical Sci-

ences Research Council. Support from the European Science Foundation (ESF) within the activity ‘New Trends and Applications of the Casimir Effect’ is gratefully acknowledged.

#### Appendix A: Limits and their leading corrections

To calculate the CP potential in the perfect-conductor and non-retarded limits, we need to approximate the spherical Bessel functions for small and large arguments. Using the asymptotes from §10 of Ref. [43]

$$j_l(x) \approx \frac{\sin(x - l\pi/2)}{x} \quad \text{for } x \gg 1; \quad (A1)$$

$$h_l^{(1)}(x) \approx \frac{(-i)^{l+1} e^{i(x - n\pi/2)}}{x} \quad \text{for } x \gg 1, \quad (A2)$$

we easily find the perfect-conductor limits (3.4) and (3.5).

The non-retarded limits (3.6), (3.7), (3.8) and (3.9) can be found by using the expansions [43]

$$j_l(x) = \frac{x^l}{(2l+1)!!} \left[ 1 - \frac{x^2}{2(2l+3)} + \dots \right] \quad (A3)$$

$$h_l^{(1)}(x) = -\frac{i(2l-1)!!}{x^{l+1}} \left[ 1 + \frac{x^2}{2(2l-1)} + \dots \right] \quad (A4)$$

for  $x \ll 1$  with  $(2l+1)!! = 1 \cdot 3 \cdot 5 \dots (2l+1)$ . Note that the next-to-leading order expansion is only needed for (3.8), where the leading-order term vanishes.

##### 1. Retardation corrections

To calculate the retardation correction to the perfect-conductor  $TM$ -mode reflection coefficients (3.5), we use the expansions (A3) and (A4), which together with the definitions (3.2) lead to

$$\tilde{j}'_l(x) = \frac{(l+1)x^l}{(2l+1)!!} \left[ 1 - \frac{x^2}{2} \frac{l+3}{(2l+3)(l+1)} + \dots \right] \quad (A5a)$$

$$\tilde{h}_l^{(1)'}(x) = \frac{il(2l-1)!!}{x^{l+1}} \left[ 1 + \frac{x^2}{2} \frac{l-2}{l(2l-1)} + \dots \right] \quad (A5b)$$

for  $x \ll 1$ . This immediately yields Eq. (3.15).

The retardation correction from the propagator factors are found from expansions

$$h_l^{(1)}(x)^2 = -\frac{[(2l-1)!!]^2}{x^{2l+2}} \left[ 1 + \frac{x^2}{2l-1} + \dots \right]; \quad (A6a)$$

$$\tilde{h}_l^{(1)'}(x)^2 = -\frac{l^2[(2l-1)!!]^2}{x^{2l+2}} \left[ 1 + \frac{x^2(l-2)}{l(2l-1)} + \dots \right] \quad (A6b)$$

which follow from Eqs. (A4) and (A5b). Combining these results with  $r_{l,0}^{\text{TM,PC}}$  as given by Eq. (3.7), we arrive at Eq. (3.16).

Expansion (A6a) moreover combines with  $r_{l,0}^{\text{TE,PC}}$  as given by Eq. (3.6) to result in Eq. (3.17).



## 2. Finite reflectivity correction

In order to expand the reflection coefficients (3.3) in powers of  $\varepsilon^{-1}$ , we rewrite them as

$$r_l^{\text{TM}}(\phi x) = r_l^{\text{TM,PC}}(\phi x) \frac{1 - AJ/\varepsilon}{1 - AH/\varepsilon};$$

$$r_l^{\text{TE}}(\phi x) = r_l^{\text{TE,PC}}(\phi x) \frac{1 - 1/(AJ)}{1 - 1/(AH)}$$

where

$$A = \frac{\tilde{j}_l'(\sqrt{\varepsilon}\phi x)}{\tilde{j}_l(\sqrt{\varepsilon}\phi x)}; \quad J = \frac{j_l(\phi x)}{\tilde{j}_l(\phi x)}; \quad H = \frac{h_l^{(1)}(\phi x)}{\tilde{h}_l^{(1)'}(\phi x)}.$$

With the assumption  $\text{Im}\{\sqrt{\varepsilon}\}\phi x \gg 1$ , the asymptote (A1) leads to

$$\frac{\tilde{j}_l'(\sqrt{\varepsilon}\phi x)}{\tilde{j}_l(\sqrt{\varepsilon}\phi x)} \approx \sqrt{\varepsilon}\phi x \cot(\sqrt{\varepsilon}\phi x - \frac{l\pi}{2}) \approx -i\sqrt{\varepsilon}\phi x.$$

Using the asymptotes (A3) and (A4), we further have

$$\frac{j_l(\phi x)}{\tilde{j}_l(\phi x)} \approx \frac{1}{l+1}; \quad \frac{h_l^{(1)}(\phi x)}{\tilde{h}_l^{(1)'}(\phi x)} \approx -\frac{1}{l}$$

for  $x \ll 1$ . Combining these results and retaining only the next-to-leading order in  $x$ , one easily obtains Eqs. (3.23).

### Appendix B: Casimir-Polder expression for a dielectric sphere

An expression for the CP potential on a particle near a dielectric sphere can be readily derived using the same methods as elsewhere in this article. Although it may be written in closed form in terms of hypergeometric functions, this hardly constitutes a simplification, and we will only give the expression as an infinite sum. The sphere's dielectric constant  $\varepsilon$  is now no longer assumed large, so that  $|\sqrt{\varepsilon}|x \ll 1$  is assumed. The TE contribution is now of order  $x^4$  and can be neglected. Since we are considering frequencies  $\omega_{kn}$  which are typically small on an optical scale, we assume  $\varepsilon(\omega_{kn}) = \varepsilon(0) = \varepsilon$ . The result is

$$U_{nk}^{\text{diel.}} \approx - \frac{|\mathbf{d}_{kn}|^2(\varepsilon - 1)}{24\pi\varepsilon_0 r^3} \sum_{l=1}^{\infty} \frac{l(l+1)(2l+1)\phi^{2l+1}}{\varepsilon l + l + 1} \times \left\{ 1 + 2x^2 \left( \frac{k_B T}{\hbar\omega_{kn}} + \frac{1}{2} \right) \left[ \frac{1}{2l+1} - \frac{\phi^2(2l+1)}{(2l-1)(2l+3)} \frac{\varepsilon(l-2) + l + 1}{\varepsilon l + l + 1} \right] \right\}. \quad (\text{B1})$$

Eq (B1) is the counterpart of (1.5) for the case of a dielectric sphere.

As for the case of a metal sphere, the approximation is good to at least the 1% level at all temperatures when  $x \lesssim 0.01$ , and becomes significantly better

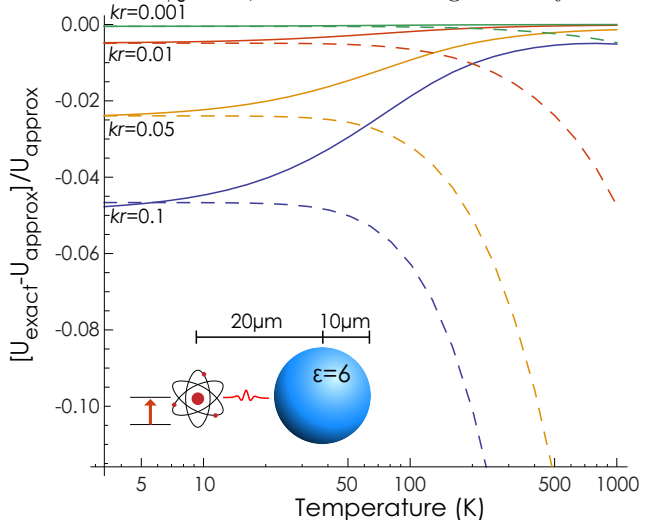


FIG. 5: Numerical comparison of the exact CP potential  $U(T)$  of a two-level model particle (transition energy  $\hbar ck$ ) outside a dielectric sphere with the approximation Eq. (B1) with (solid line) and without (dashed lines) the correction term in the curly brackets. Parameter values:  $R = \frac{1}{2}r = 10\mu\text{m}$  and  $\varepsilon = 6$ .

for  $T \gg \hbar\omega/k_B$  (about 11K for  $x = 0.01$  with the numbers in figure 5).

When assuming as we have that  $\varepsilon$  does not vary appreciably between frequencies 0 and  $\omega_{kn}$ , the leading order correction is of order  $x^2$ . It is noteworthy that the T-independent term alone (without the correction in the curly braces of Eq. (B1)) is about as good an approximation as the corresponding expression is for a metal sphere. This conclusion would not hold, however, if the dielectric material has resonances at frequencies in the order of  $\omega$ , which might lie in the microwave or far infrared regime, in which case  $\Delta\Gamma_\omega$  may no longer be small compared to  $\Gamma_0$  (see Section II).

[1] H. B. G. Casimir and D. Polder, Phys. Rev. **73**, 360 (1948).

[2] T. F. Gallagher, *Rydberg Atoms* (Cambridge University

- Press, 1994).
- [3] H. Kübler, J. P. Shaffer, T. Baluktsian, R. Löw, and T. Pfau, *Nature Photonics* **4**, 112 (2010).
  - [4] A. Tauschinsky, R. M. T. Thijssen, S. Whitlock, H. B. van Linden van den Heuvell, and R. J. C. Spreeuw, *Phys. Rev. A* **81**, 063411 (2010).
  - [5] A. S. Sørensen, C. H. van der Wal, L. I. Childress, and M. D. Lukin, *Phys. Rev. Lett* **92**, 063601 (2004).
  - [6] P. Hyafil, J. Mozley, A. Perrin, J. TAILLEUR, G. Noguez, M. Brune, J. M. Raimond, and S. Haroche, *Phys. Rev. Lett* **93**, 103001 (2004).
  - [7] D. Petrosyan, G. Bensusky, G. Kurizki, I. Mazets, J. Majer, and J. Schmiedmayer, *Phys. Rev. A* **79**, 040304(R) (2009).
  - [8] S. Y. T. van de Meerakker, H. L. Bethlem, and G. Meijer, *Nature Physics* **4**, 595 (2008).
  - [9] L. D. Carr, D. DeMille, R. V. Krems, and J. Ye, *New J. Phys.* **11**, 055049 (2009).
  - [10] M. T. Bell and T. P. Softley, *Mol. Physics* **107**, 99 (2009).
  - [11] S. A. Meek, H. Conrad, and G. Meijer, *Science* **324**, 1699 (2009).
  - [12] A. Ashkin, *Phys. Rev. Lett.* **24**, 156 (1970).
  - [13] J. Chen, J. Ng, Z. Lin, and C. T. Chan, *Nature Photonics* **5**, 531 (2011).
  - [14] S. Kawata and T. Sugiura, *Opt. Lett* **17**, 772 (1992).
  - [15] S. M. Spillane, T. J. Kippenberg, and K. J. Vahala, *Nature* **415**, 621 (2002).
  - [16] H. Haakh, F. Intravaia, C. Henkel, S. Spagnolo, R. Passante, B. Power, and F. Sols, *Phys. Rev. A* **80**, 062905 (2009).
  - [17] S.Y. Buhmann, M.R. Tarbutt, S. Scheel, and E.A. Hinds, *Phys. Rev. A* **78**, 052901 (2008).
  - [18] J. A. Crosse, S. Å. Ellingsen, K. Clements, S. Y. Buhmann, and S. Scheel, *Phys. Rev. A* **82**, 010901(R) (2010); Erratum *ibid.* **82**, 029902(E) (2010).
  - [19] S. Y. Buhmann and S. Scheel, *Phys. Rev. Lett.* **100**, 253201 (2008).
  - [20] S. Å. Ellingsen, S. Y. Buhmann, and S. Scheel, *Phys. Rev. A* **79**, 052903 (2009).
  - [21] S. Å. Ellingsen, S. Y. Buhmann, and S. Scheel, *Phys. Rev. Lett.* **104**, 223003 (2010).
  - [22] S. Å. Ellingsen, S.Y. Buhmann, and S. Scheel, *Phys. Rev. A* **84**, 060501(R) (2011).
  - [23] T. Nakajima, P. Lambropoulos and H. Walther, *Phys. Rev. A* **56**, 5100 (1997).
  - [24] S.-T. Wu and C. Eberlein, *Proc. R. Soc. Lond. Ser. A* **456**, 1931 (2000).
  - [25] M.-P. Gorza and M. Ducloy, *Eur. Phys. J. D* **40**, 343 (2006).
  - [26] M. Antezza, L. P. Pitaevskii, S. Stringari, and V. B. Svetovoy, *Phys. Rev. A* **77**, 022901 (2008).
  - [27] Y. Sherkunov, *Phys. Rev. A* **79**, 032101 (2009).
  - [28] S. Y. Buhmann and D.-G. Welsch, *Prog. Quantum Electron.* **31**, 51 (2007).
  - [29] S. Scheel and S. Y. Buhmann, *Acta Phys. Slov.* **58**, 675 (2008).
  - [30] S. Å. Ellingsen, Y. Sherkunov, S.Y. Buhmann, and S. Scheel, in *Proceedings of the Ninth Conference on Quantum Field Theory Under the Influence of External Conditions (QFEXT09)* edited by M. Bordag and K. A. Milton (World Scientific, 2010), p. 168, Preprint: [quant-ph/0910.5608](#).
  - [31] A. Weber and H. Gies, *Phys. Rev. Lett.* **105**, 040403 (2010).
  - [32] T. L. Ferrell and R. H. Ritchie, *Phys. Rev. A* **21**, 1305 (1980).
  - [33] A. M. Marvin and F. Toigo, *Phys. Rev. A* **25**, 782 (1982); **25**, 803 (1982).
  - [34] C. Girard, S. Maghezzi, and F. Hache, *J. Chem. Phys.* **91**, 5509 (1989).
  - [35] W. Jhe and J. W. Kim, *Phys. Rev. A* **51**, 1150 (1995).
  - [36] V. V. Klimov, M. Ducloy, and V.S. Letokhov, *J. Mod. Opt.* **43**, 2251 (1996).
  - [37] S. Y. Buhmann, H. T. Dung, and D.-G. Welsch, *J. Opt. B: Quantum Semiclass. Opt.* **6**, S127 (2004); Erratum: *J. Phys. B: At. Mol. Opt. Phys.* **39**, 3145 (2006).
  - [38] M. M. Taddei, T. N. C. Mendes and C. Farina, *Eur. J. Phys.* **31**, 89 (2010).
  - [39] A. Sambale, S. Y. Buhmann, and S. Scheel, *Phys. Rev. A* **81**, 012509 (2010).
  - [40] M. Babiker and G. Barton, *J. Phys. A: Math. Gen.* **9**, 129 (1976).
  - [41] I. Brevik, S. A. Ellingsen and K. A. Milton, *New J. Phys.* **8**, 236 (2006).
  - [42] S. Y. Buhmann, S. Scheel and J. Babington, *Phys. Rev. Lett.* **104**, 070404 (2010).
  - [43] M. Abramowitz and I. A. Stegun, *Handbook of Mathematical Functions* (Dover, New York, 1964).